

Microphase separation and liquid-crystalline ordering of rod-coil copolymers

A. AlSunaidi,^{1,a)} W. K. den Otter,^{2,b)} and J. H. R. Clarke^{3,c)}

¹Department of Physics, King Fahd University of Petroleum and Minerals, Dhahran 31261, Saudi Arabia

²Faculty of Science and Technology, University of Twente, P.O. Box 217, 7500 AE Enschede, The Netherlands

³School of Chemistry, University of Manchester, P.O. Box 88, Manchester M60 1QD, United Kingdom

(Received 27 November 2008; accepted 27 January 2009; published online 27 March 2009)

Microphase separation and liquid-crystalline ordering in diblock and triblock rod-coil copolymers (with rod-to-coil fraction $f=0.5$) were investigated using the dissipative particle dynamics method. When the isotropic disordered phases of these systems were cooled down below their order-disorder transition temperatures T_{ODT} , lamellar structures were observed. For rod-coil diblock copolymers, the lamellar layers were obtained below $T=2.0$. This temperature was found to be higher than the T_{ODT} for normal coil-coil diblock copolymers. Significant ordering of the rods was observed only below $T=0.9$ which is the isotropic-nematic transition temperature for rodlike fluids. For the triblock rod-coil copolymers, both microphase separation and rod ordering occurred at $T=0.9$. Normal coil-coil triblock copolymers were found to undergo microphase separation at $T=0.8$, which is about half the T_{ODT} of the normal diblock copolymers. Investigations of the mean square displacement and the parallel and the perpendicular components of the spatial distribution function revealed that at low temperatures, the rod-coil diblock copolymers exhibit smectic-A and crystalline phases, while the triblock copolymers show smectic-C and crystalline phases. No nematic phases were observed at the density and interaction parameters used in this study. © 2009 American Institute of Physics. [DOI: [10.1063/1.3089701](https://doi.org/10.1063/1.3089701)]

I. INTRODUCTION

Self-assembly in copolymers made of flexible (coil) blocks has been a topic of high importance in the past decade. It occurs as a result of incompatibility between the blocks, which leads to microphase separation. In order to understand the phase behavior of melts of coil-coil multi-block copolymers, researchers have investigated the phase behavior of the simplest units, namely, the diblock and the triblock copolymers.^{1,2} These two architectures show similar morphologies once they undergo microphase separation with little asymmetry in the phase diagram of the triblock.² Moreover, it was found experimentally³ that diblock and triblock copolymers with the same length and the same composition have different order-disorder transition (T_{ODT}) temperatures because of reduced conformational entropy of the triblock copolymer as the ends of the middle block have to be located at a domain boundary. Consequently, the disordered phase of a triblock copolymer melt at high temperatures is more stable than that of a diblock copolymer of the same length and composition. The quantity of major importance in determining the microphase separation temperature is the product of the Flory–Huggins parameter χ and the length N of the copolymer chain defined by the number of segments of given reference volume. Mayes and Olvera de la Cruz⁴ obtained a

critical value for microphase separation of $(\chi N)_c \approx 18$ for melts of symmetrical triblock copolymers compared to a value of $(\chi N)_c \approx 10.5$ for melts of diblock copolymers of the same length and composition.

Recently, more attention has been given to rod-coil block copolymers composed of rigid blocks bonded to flexible chains.⁵ These molecules could produce novel electronic, optoelectronics, and optical devices, and could serve as synthetic analogs of proteinlike molecules and to the design of new types of biomimetic materials. Self-assembly in these systems is not only driven by the microphase separation between the incompatible blocks but also by the liquid-crystalline ordering of the rods. The competition between these two processes could increase the number of possible phase-separated morphologies observed in the coil-coil copolymers, and allow access to structures with smaller length scales not attainable with normal coil-coil copolymers. One of the early experimental investigations of self-assembly in rod-coil copolymer (poly(hexyl-isocyanate-*b*-stryne)) melts was carried out by Chen *et al.*⁶ The morphologies found were all lamellar with the rods forming tilted smectic phases. The size of the domains was ranging from tens of nanometers to almost one micrometer. As the coil-to-rod ratio, f is decreased, the lamellar observed were wavy, zig-zag, and arrowhead. Following this, Jenekhe and Chen⁷ demonstrated that amphiphilic poly(phenylquinoline)-polystyrene rod-coil diblock copolymers self-organize into micrometer-scale spherical, vesicular, cylindrical, and lamellar aggregates from solution depending on volume fraction of the rods, and the aggregates are about two orders of magnitude larger than the

^{a)}Electronic mail: asunaidi@kfupm.edu.sa.

^{b)}Electronic mail: w.k.denotter@utwente.nl.

^{c)}Electronic mail: jhrc@manchester.ac.uk.

coil-coil block copolymer micelles. Self-assembly in rod-coil triblock copolymers was also investigated experimentally. Rubatat *et al.*,⁸ for example, observed lamellar layers with tilted rods at different coil volume fractions of PBLG-PHF-PBLG copolymers. A series of liquid-crystalline phases ranging from lamellar crystalline and bicontinuous cubic to body central tetragonal phases were observed by Lee *et al.*⁹ as the coil ratio in rod-coil diblock and triblock copolymers is increased.

Theoretically, Matsen and Barrett¹⁰ applied a self-consistent density functional method to understand the self-assembly in rod-coil diblock copolymers. Three parameters were used in their study: χN , f and a parameter, v , representing the ratio of the coil volume to the rod volume. Taking the nematic phase to be the high temperature phase, they obtained smectic-A and smectic-C phases. Reenders and ten Brinke¹¹ derived a Landau free energy functional to investigate the phase behavior of rod-coil diblock copolymers. They obtained phase diagrams that depend on three parameters, χN , f and the Maier-Saupe parameter ω , which represents the steric repulsion between rods. Nematic and smectic-C phases were obtained, but with no evidence of smectic-A phase in the phase diagram. Self-consistent mean-field calculations made by Duchs and Sullivan¹² and Hidalgo *et al.*¹³ to study liquid-crystalline phases of rod-coil copolymers resulted in nematic and smectic-A phases upon increasing the density with no repulsive Flory interactions χ , between the rod and the coil blocks. Chen *et al.*¹⁴ made a comparison of the phase diagram of rod-coil diblock and triblock copolymers by applying a self-consistent field lattice method. They observed that the stability of the lamellar phase and the order-disorder transition point depend of the structure of the copolymer.

This work presents a comparison in the self-assembly of rod-coil diblock and rod-coil triblock copolymers of the same length N and composition (with rod-to-coil volume fraction $f=0.5$) using computer simulation. We will be investigating the effect of adding the flexible tails on the liquid-crystalline properties of rodlike fluids, and the effect of the rigidity of one block on the microphase separation (or χ) of normal coil-coil copolymers. These aspects of self-assembly in rod-coil copolymers were not investigated in reported simulations.^{15–25} In a previous paper,²⁶ we reported the first attempt to use the dissipative particle dynamics (DPD) simulation method, with its soft potential, to investigate the liquid-crystalline ordering in rodlike and rod-coil fluids. It is now well established that methods based on soft potentials^{26–28} provide rapid equilibration and give qualitatively the expected physics for interacting particles. For this reason we continue to use the DPD in the present study. The organization of this paper is as follows: in Sec. II, the DPD simulation method and the copolymer models studied will be described. The results of our simulations for the rod-coil copolymer diblock and the triblock models will be presented in Sec. III. Finally, conclusions are given in the last section.

II. SIMULATION METHOD

To simulate the rod-coil systems at a mesoscale level, we used the dissipative particle dynamics (DPD) method. The DPD is a particle-based simulation technique in which particles interact via soft potentials and is well suited to the study of mesoscale phenomena. In this method, every particle represents a collection of atoms, just like the beads in a bead-spring model of a polymer. The net force applied on particle i is a sum of three pairwise additive forces:

$$\mathbf{f}_i = \sum_{j \neq i} \mathbf{f}_{ij}^C + \sum_{j \neq i} \mathbf{f}_{ij}^D + \sum_{j \neq i} \mathbf{f}_{ij}^R, \quad (1)$$

where the sums run over all neighboring particles j within a cutoff distance $r_c=1$. The first force is a conservative force,

$$\mathbf{f}_{ij}^C = a_{ij} \omega_C(r_{ij}) \hat{\mathbf{r}}_{ij}, \quad (2)$$

where a_{ij} sets the strength of the potential, $\omega_C(r_{ij})=1-|r_{ij}|/r_c$, gives the shape of the potential, and $r_{ij}\hat{\mathbf{r}}_{ij}=\mathbf{r}_i-\mathbf{r}_j$ with the hat denoting a unit vector. In our simulations, we will define a_{CC} , a_{RR} and a_{CR} to represent the strength of the repulsion between the coil-coil, rod-rod, and coil-rod species, respectively.

Since a DPD particle represents a collection of many atoms, averaging over the internal degrees of freedom gives rise to a dissipative (or friction) force

$$\mathbf{f}_{ij}^D = -\gamma \omega_D(r_{ij}) (\hat{\mathbf{r}}_{ij} \cdot \mathbf{v}_{ij}) \hat{\mathbf{r}}_{ij}, \quad (3)$$

and a random (or stochastic) force

$$\mathbf{f}_{ij}^R = \sigma \omega_R(r_{ij}) \theta_{ij}(t) \hat{\mathbf{r}}_{ij}. \quad (4)$$

Here, γ is the friction coefficient, σ controls the magnitude of the random force, and ω_D and ω_R give the distance dependence of these two contributions with $\omega_D=\omega_R^2=(1-r)^2$. The random number $\theta_{ij}(t)$ has zero average, unit variance, differs for each particle pair and varies in time without memory, i.e., $\langle \theta_{ij}(t) \theta_{kl}(t') \rangle = (\delta_{ik} \delta_{jl} + \delta_{il} \delta_{jk}) \delta(t-t')$. The balance between the random and the friction forces provides the thermostat with the condition that

$$\sigma^2 \omega_R^2(r) = 2\gamma \omega_D(r) k_B T, \quad (5)$$

where k_B is the Boltzmann constant and T is the temperature.

The dynamics of the DPD particles are followed by solving Newton's equation of motion, with the above forces, by means of the Verlet leap frog algorithm.²⁹ In the simulation we choose the mass of the particles and the cutoff radius as the units of mass and distance, respectively. The conservative force constant, the temperature (henceforth we will use "temperature" to refer to $k_B T$), and other energy-dependent quantities are expressed in multiples of the unit of energy. We selected a time step of $\delta t=0.04$. At this value of the time step, the inaccuracies in the integration of the friction and random forces lead to a kinetic temperature, $T_{\text{kin}}=3m\langle \mathbf{v}_i^2 \rangle$, only moderately higher than the desired temperature.^{29,30}

In our simulations, the rods are modeled as seven fused spheres. The distance between consecutive spheres is fixed at $2r_c/3$ so that the length-to-width ratio of our rods is about 5. During the simulation, the standard SHAKE routine is used to keep the two end particles of the rod at a fixed distance.³¹

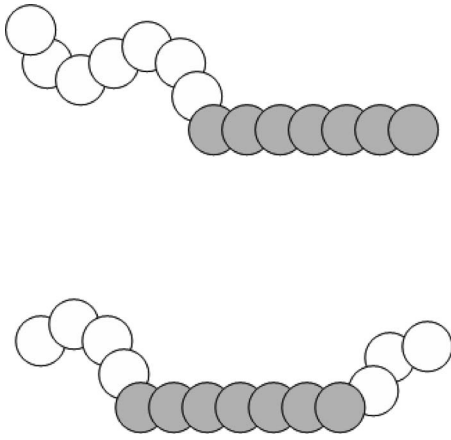


FIG. 1. Schematics of the rod-coil diblock (up) and triblock (down) copolymers.

The positions of the five intermediate particles are then readily calculated by a linear interpolation at the end of each time step. The flexible coil is modeled as a chain of several DPD particles. Adjacent spheres are connected by harmonic springs, $f_{ij}^S = C(r_{ij} - r_0)$, with the equilibrium distance $r_0 = 2r_c/3$ and the spring constant $C = 4$. This value of C was chosen in order to keep the bonds between the coil particles always close to r_0 .

Our simulations were carried out at constant pressure and temperature (NPT ensemble) using the Berendsen barostat³² and the DPD thermostat. A constant pressure routine allowed all box dimensions to change independently, minimizing the effect of the box size and shape on the final equilibrium structure. The diagonal elements of the pressure were fixed to 30, while setting the nondiagonal elements to zero. To obtain any desired temperature, we opted to keep the friction constant at $\gamma = 2.66$, while varying σ . This choice has the physically appearing advantage of making both $(\mathbf{f}_{ij}^D)^2$ and $(\mathbf{f}_{ij}^R)^2$ scale linearly with temperature. The initial box has dimensions $22 \times 22 \times 22$, with periodic boundary conditions applied in all directions. For each of the rod-coil copolymer systems, we simulated 3000 copolymers each with 14 DPD particles giving a sample size of 42 000 particles. Figure 1 shows the models for the copolymers used in this study. The diblock consists of two blocks (rod and coil: A_7B_7) each of seven particles. The triblock is composed of two end chains (of three and four particles: $A_4B_7A_3$) connected to a rod of seven particles placed in the middle. The rodlike fluid is made of rigid blocks each of seven particles. The coil-coil copolymers are similar to the rod-coil ones except that the rod block is made flexible.

III. RESULTS AND DISCUSSION

The simulations were carried out by initially placing the copolymers at random in a cubic box followed by equilibration at a high temperature with the coil-coil, rod-rod, and rod-coil repulsion parameters set to $a_{CC} = a_{RR} = a_{RC} = 20$. This resulted in a highly disordered, mixed system. In order to see microphase separation, the copolymer systems were then quenched to a temperature of $T = 0.7$, and simultaneously the rod-coil repulsion was increased to $a_{RC} = 25$. This value of

a_{RC} corresponds roughly to $\chi N \approx 48$,²⁶ which is larger than the $(\chi N)_c$ for normal coil-coil diblock and triblock copolymers.⁴ This puts the system in the intermediate segregation regime of the phase diagram. After that series of cooling and heating runs were carried out to determine the T_{ODT} and the clearing point (isotropic-smectic in this case) for each system.

In order to investigate the competition between microphase separation and liquid-crystalline ordering of the copolymers we have calculated two quantities that would give information about the variation of the structure of the system as a function of temperature. Microphase separation is identified whenever the isotropic mixed system starts to show some anisotropy in its structure as the temperature is lowered. To find the T_{ODT} , microphase separation was monitored by calculating the structure factors

$$S_R(\mathbf{k}) = \frac{1}{N_R} \left\langle \left[\sum_{i=1}^{N_R} \sin(\mathbf{k} \cdot \mathbf{r}_i) \right]^2 + \left[\sum_{i=1}^{N_R} \cos(\mathbf{k} \cdot \mathbf{r}_i) \right]^2 \right\rangle, \quad (6)$$

where the sums run over all N_R rod particles. Analogous to the principal moments of inertia for mass distribution in classical mechanics, we calculated the eigenvalues of the matrix $\int \mathbf{k} S_R(\mathbf{k}) \mathbf{k} d\mathbf{k}$ and sorted them by value to obtain the principal moments $\lambda_1 \leq \lambda_2 \leq \lambda_3$ of the structure factors. Symmetry breakdown accompanying T_{ODT} can then be characterized by two invariants,³³ $Q_1 = (\lambda_2 + \lambda_3)/\lambda_1 - 2$ and $Q_2 = (\lambda_3 - \lambda_2)/\lambda_1$. The latter remained close to zero at all temperatures, while Q_1 is expected to be zero for isotropic structures and nonzero for microphase separated structures. Similarly, liquid-crystalline ordering was monitored by calculating the orientational order parameter, S_2 . This is done by evaluating the matrix

$$\mathbf{Q} = \frac{1}{2} (3 \langle \hat{\mathbf{u}}_i \hat{\mathbf{u}}_i \rangle - \mathbf{1}), \quad (7)$$

where $\hat{\mathbf{u}}_i$ is the unit vector parallel to the i th rod. The order parameter S_2 is the largest (positive) eigenvalue of this matrix; the corresponding eigenvector $\hat{\mathbf{n}}$ is called the director, as it points in the average direction of the rods. Order is measured here as the width of the distribution of $\hat{\mathbf{u}}_i$ around $\hat{\mathbf{n}}$, and runs from zero for randomly oriented rods to one for perfectly oriented rods.

A plot of Q_1 values for the rod-coil diblock copolymers as a function of temperature is shown in Fig. 2. In order to study the effect of block rigidity on the T_{ODT} , we also show in the same figure a plot of Q_1 values for normal coil-coil (AB) diblock copolymers composed of two incompatible ($a_{AA} = 20$, $a_{BB} = 20$, and $a_{AB} = 25$) flexible coils made of seven DPD particles. For the rod-coil copolymers, Q_1 is above unity (and almost constant) for low T indicating the formation of microphase separated structures. Above $T \approx 1.0$, Q_1 drops gradually and reaches zero (T_{ODT} for the rod-coil diblock copolymers) at $T \approx 2.0$. We have observed from visualization (see Fig. 3) that in the temperature range from $T = 0.1$ up to $T \approx 0.7$, the copolymers form perfect lamellar structures. The fluctuations observed in Q_1 between

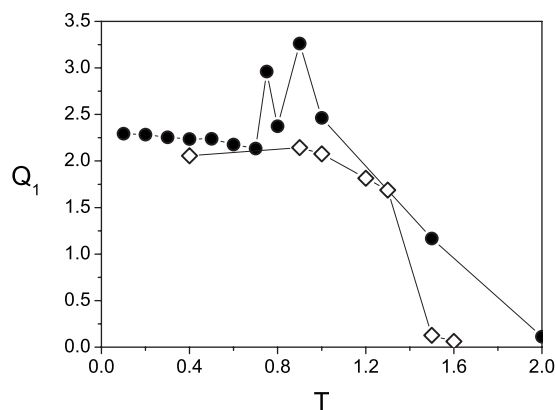


FIG. 2. The variation of Q_1 with temperature for the rod-coil (circle) and coil-coil (diamond) diblock copolymers.

$T=0.7$ and $T=1.0$ are resulting from the frustration in the lamellae as the rods suddenly start losing their orientational order. Above $T \approx 1.0$ and up to the T_{ODT} , perforations in the lamellar structure (broken lamellae) start to develop, as shown in Fig. 3(b). Perforations were not seen in the normal diblock copolymers but perfect lamellar layers were observed. Q_1 values for the normal coil-coil copolymer are nonzero at low T . As T increases beyond 1.2, Q_1 falls sharply and reaches zero (T_{ODT}) at $T \approx 1.5$. Comparing the T_{ODT} of the rod-coil to the coil-coil diblock copolymers, it is clear that the phase diagram (at $f=0.5$) shifts toward lower values of the Flory parameter χ (higher values of T) as one of the coils become rigid.

We have also investigated the orientational ordering of the rods using Eq. (7). A plot of S_2 as a function of temperature, for the rods belonging to the rod-coil copolymer is shown in Fig. 4. Also plotted in the same figure the values of S_2 as a function of temperature for the pure rodlike fluid. Below $T=0.4$, the values of S_2 for both systems are close to unity. Above this temperature, the rodlike fluid shows a sharp smectic to nematic transition as the value of S_2 jumps from about 0.98 to 0.9. There is no such transition in the rod-coil copolymers where they keep their values of S_2 larger than those of the rod system up to $T=0.7$ after which S_2 starts decreasing sharply. At $T \approx 0.9$, the rodlike fluid undergoes a nematic-isotropic transition where S_2 drops sharply to zero (clearing point) while the rod-coil copolymers still keep a noticeable ordering ($S_2=0.25$) at this temperature. Between $T \approx 0.7$ and $T \approx 1.0$, the value of S_2 for the rod-coil copolymers drops sharply from $S_2 \approx 0.9$ to $S_2 \approx 0.1$. This is the same temperature range where we have seen fluctuations in the value of Q_1 . The small residual value of S_2 then decreases smoothly before it reaches zero at $T \approx 2.0$, which is almost equal to the T_{ODT} of the rod-coil diblock copolymer when microphase separation completely fades out. The fact that the rods in the rod-coil copolymers are forced by the microphase separation to stay in layers prevents the system from showing a nematic phase.

A similar approach is now applied to the rod-coil triblock copolymers. Figure 5 shows plots of Q_1 values for the rod-coil and the normal coil-coil triblock copolymers. The T_{ODT} for the normal triblock copolymers occurs at $T \approx 0.8$, lower than that of the rod-coil triblock copolymers which

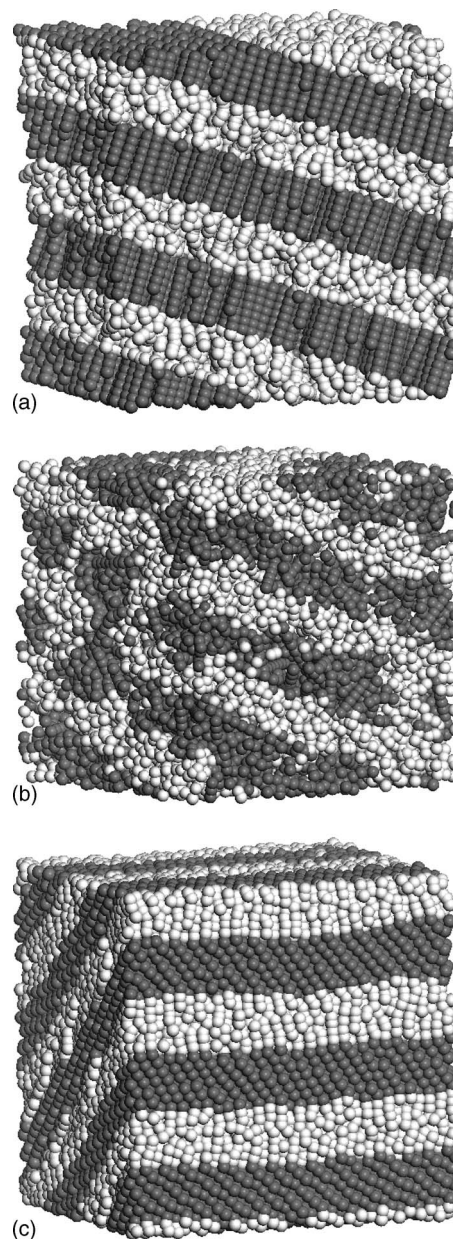


FIG. 3. Snapshots for the microphase separated (a) diblock rod-coil copolymers at $T=0.1$, (b) diblock rod-coil copolymer at $T=1.5$, and (c) triblock rod-coil copolymers at $T=0.1$. Rods are in dark color and coils are in light color.

occurs at $T \approx 0.9$. Looking also at the behavior of S_2 , shown in Fig. 6, we notice that just like the rod-coil diblock copolymers, the rod-coil triblock copolymers do not exhibit a smectic-nematic transition. What is interesting is that unlike the rod-coil diblock, the triblock exhibit a sharp smectic-isotropic transition at the clearing point of the rodlike fluid. Also, the T_{ODT} and the smectic-isotropic transition for the rod-coil triblock copolymers occur at the same temperature $T \approx 0.9$, which is also the clearing point for the rodlike fluid. A snapshot for the layers formed by the rod-coil triblock copolymers at $T=0.1$ is shown in Fig. 3(c).

There is a good agreement between the above findings and the reported experimental and theoretical calculations. It is found experimentally³ and theoretically⁴ that the normal diblock copolymers are more stable in the ordered lamellar

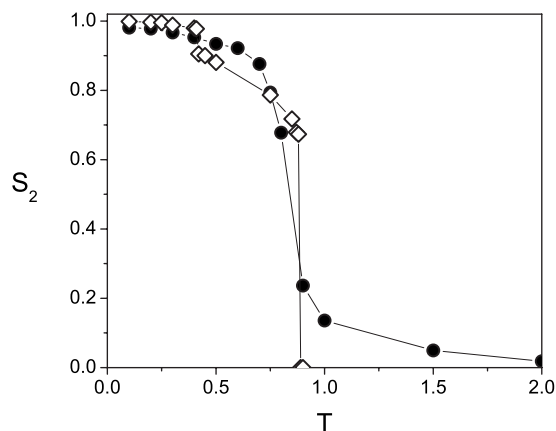


FIG. 4. The variation of the orientational order parameter S_2 for the rod-coil diblock copolymer (circle) and the rodlike fluid (diamond).

phase than the triblock counterparts. We have proven this in our DPD calculations where we have shown that the T_{ODT} for the normal diblock copolymers is about twice that of the normal triblock copolymers. We have also shown that this is also true for rod-coil copolymers by finding that the T_{ODT} for the rod-coil diblock copolymers is about twice that of the rod-coil triblock copolymers. Moreover, we have shown that the existence of a rigid block in the copolymer increases the T_{ODT} (decreases χ). This agrees with the theoretical prediction by Matsen³⁴ that the increase in the molecular rigidity of melts of semiflexible diblock copolymers moves the order-disorder transition to higher temperatures. Our work also agrees with the experimental work of Lee *et al.*⁹ who obtained a lamellar structure of rod-coil triblock copolymers at $f=0.47$. It however contradicts the theoretical results of Chen *et al.*¹⁴ who predicted a stable lamellar structure for the triblock copolymers only at $f=0.8$.

We have also investigated the liquid-crystalline phases made by the two rod-coil copolymers. Knowing that the rod-coil copolymers do not show nematic phases at the selected density ρ , repulsion parameters a_{ij} , volume fraction f , and length-to-width ratio of the rods, then what are the phases made by these two copolymers? To answer this question we will first look at the parallel component of the pair distribution function, $g_{\parallel}(r_{\parallel})$, which represents the projection of the

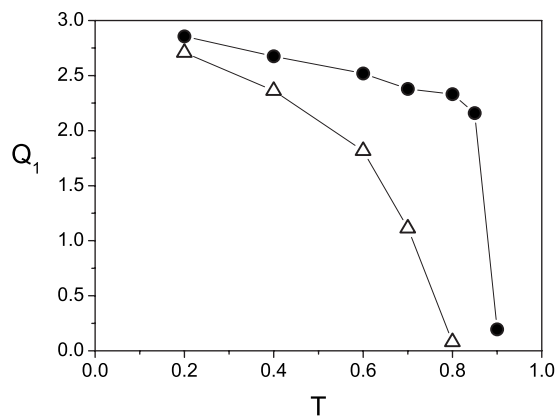


FIG. 5. The variation of Q_1 with temperature for the rod-coil (circle) and coil-coil (diamond) triblock copolymers.

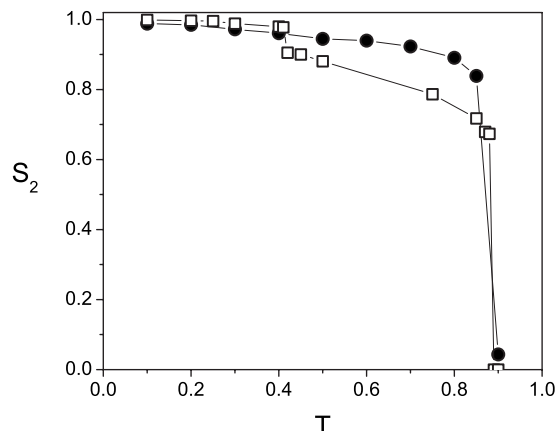


FIG. 6. The variation of the orientational order parameter S_2 for the rod-coil triblock copolymer (circle) and the rodlike fluid (square).

pair distribution function, $g(r)$ along a vector normal to the layers where r_{\parallel} is the parallel distance along the normal to the layer. Usually for one-component systems,³⁵ $g_{\parallel}(r_{\parallel})$ for layered system shows oscillatory periodic behavior and is used to give the width of the layer, d . Here, however, we would like to use it to get information about the possible variation with temperature of the width of the rods layer, d_R in a system of rod-coil copolymers. Therefore, we calculated $g_{\parallel}(r_{\parallel})$ considering only the first and the last particles in the rods. However because of the interdigitation of the rods, we would expect $g_{\parallel}(r_{\parallel})$ to give two widths: d_R , which represent the parallel distance between the first and last particles across the rods layer, and d_C , which represent the parallel distance between the first and last particles along the coils layer. Plots of $g_{\parallel}(r_{\parallel})$ at $T=0.1$ and 0.6 for the rod-coil diblock and triblock copolymers are shown in Fig. 7. Notice that for the diblock copolymers [Fig. 7(a)], the position of the first peak at about 4 (in units of r_c) gives the width of the rods layer d_R . This value corresponds to the center-to-center separation between the first and last particle of a rod. Note also that the position of the peak does not change with temperature. This indicates that the rods are oriented parallel to the normal to the layer. So the tilt angle between the director \hat{n} and the normal is zero, giving either crystalline or smectic-A phases in the temperature range considered. The position of the second peak at roughly 5.5 represents the separation between the end particles but across the coil layers. For the triblock copolymer, the position of the first peak at $T=0.1$ is about 3 and changes to about 2.5 at $T=0.6$. These values are less than the center-to-center separation of the first and last particles of a rod and prove that the tilt angle is not zero but it changes with temperature. In fact, we have calculated the tilt angle to be about 23° at $T=0.1$, and 52° at $T=0.6$. This tilt between the average direction of the rods (\hat{n}) and the normal to the rods layers can be clearly seen in Fig. 3(c). It implies that the triblock rod-coil copolymers exhibit either crystalline or smectic-C liquid-crystalline phases for all the temperatures below the clearing point.

Moreover, we know that rodlike fluids made of seven DPD particles show a crystalline phase for $T < 0.3$ (Ref. 26) where a noticeable jump in the value of the orientational order parameter S_2 is observed as the smectic-crystalline

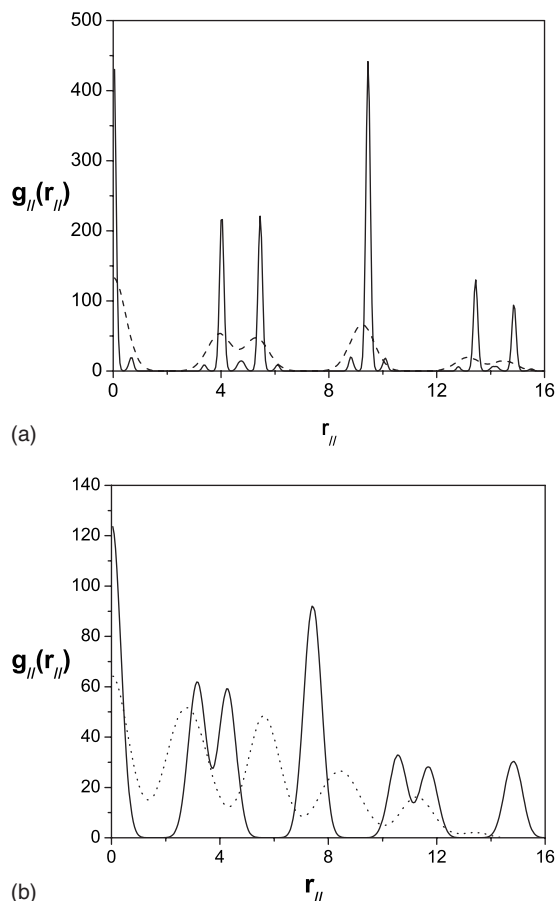


FIG. 7. The component of the radial distribution function along the director, $g_{||}(r_{||})$, at $T=0.1$ (solid) and $T=0.6$ (dashed) for rod-coil (a) diblock copolymers and (b) triblock copolymers.

transition point is crossed. For the rod-coil copolymers we did not observe sudden changes in the value of S_2 at low temperatures. However, when we investigated the time evolution of the mean square displacement, $\Delta r^2(t)$, of the central particles of the rods belonging to the diblock copolymer, we observed that $\Delta r^2(t)$ is constant at $T=0.2$ while it increases with time at $T=0.3$. This behavior of $\Delta r^2(t)$ is shown in Fig. 8. For the rod-coil triblock copolymer, we have also observed that $\Delta r^2(t)$ is constant with time when the temperature is below $T=0.4$. The constant behavior $\Delta r^2(t)$ at low temperature means that the particles are frozen in position and we, in fact, have a solid phase. Usually, the discrimination between the smectic fluidlike structure and the crystalline structure is done by calculating the in-plane positional distribution correlation function, $g_{\perp}(r_{\perp})$ which gives the correlation between the particles within the same layer.³⁵ r_{\perp} is the pair separation perpendicular to the normal to the rods plane. This function is plotted in Fig. 9 for the rods central particles of the diblock copolymer for $T=0.2$ and $T=0.3$. At the lower temperature, $g_{\perp}(r_{\perp})$ is highly structured and presents crystalline-like long-range order between the particles. At $T=0.3$, the weak positional correlation between the particles indicates a fluidlike (smectic phase) structure. The plot of $g_{\perp}(r_{\perp})$ for the triblock copolymer (not shown) exhibits similar solidlike structure at $T=0.3$ and fluidlike structure at $T=0.4$.

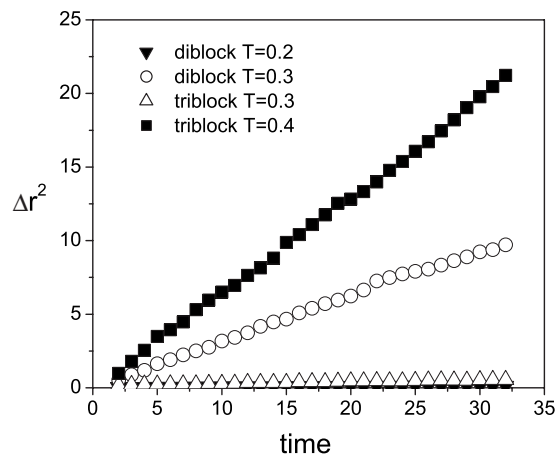


FIG. 8. The variation of the mean square displacement with simulation time for the rod-coil diblock and triblock copolymers.

The liquid-crystalline phases found here for the rod-coil diblock copolymers are in agreement with the results of the Monte Carlo simulations made by van Duijneveldt *et al.*¹⁵ who found that the nematic phase is suppressed when flexible tails (which had no volume) were attached to one end of hard spherocylinders. Similar phases were also reported by Fukunaga *et al.*¹⁶ who carried out Molecular Dynamics simulation of a system of diblock copolymers made of flexible tails attached to one end of Gay-Berne ellipsoids. Similarly for the triblock copolymers, Affouard *et al.*²⁰ conducted molecular dynamics simulation of short chains with the central part made stiff while the ends are flexible. Their $A_3B_4A_3$ chains, with attractive rigid blocks in the middle, showed a solid phase at low temperatures, followed by a smectic-A phase and then an isotropic phase at high T . Depending on the length of the flexible chain, Casey and Harrowell,²¹ showed through their on-lattice Monte Carlo simulations that coil-rod-coil copolymers could show, nematic, smectic-A, smectic-C, and solid phases. Note that in all the reported cases, the value of $f \neq 0.5$. The experimental work of Lee *et al.*⁹ also predicted a lamellar structure consisting of microphase separated crystalline rod domains and amorphous coil domains but no nematic phase.

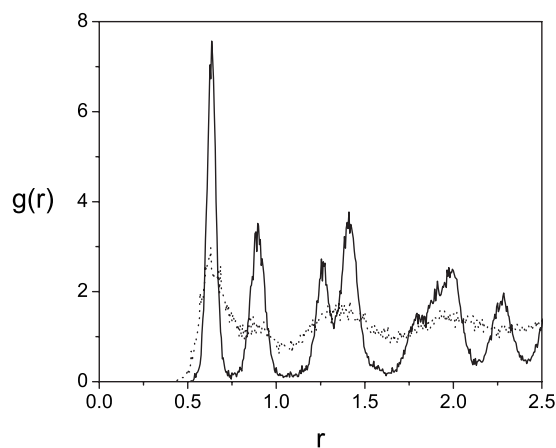


FIG. 9. The in-plane positional distribution function $g_{\perp}(r_{\perp})$ for the diblock copolymers rods central particles taken at $T=0.2$ (solid) and $T=0.3$ (dotted).

IV. CONCLUSION

The goal of this study was to provide a basic understanding of the phase behavior of the simplest building blocks of large liquid crystal molecules: the rod diblock and triblock copolymers. We used the dissipative particle dynamics simulation method that gives rapid equilibration and qualitatively the correct physics. We considered copolymers with the same $N=14$ and with rod-to-coil fraction $f=0.5$. Differences in the phase behavior of the two copolymers were found and the order-disorder temperature T_{ODT} depends strongly on the architecture of the molecule. Both copolymers form lamellar structures once they undergo microphase separation. The rod-coil diblock copolymers have higher T_{ODT} (or lower χ) than the triblock copolymers. The triblock copolymers show a sharp order-disorder transition in which the rods suddenly lose all their orientational order. However, for the diblock copolymers, perforation starts appearing in the lamellae once the rods lose their orientation, but the transition to the disordered phase occurs smoothly. We have also compared the phase behavior to normal copolymers. In general, the rod-coil copolymers have higher T_{ODT} than the normal copolymers. These observations are in agreement with reported experiments and theories of rod-coil copolymers.

We have also looked into the liquid-crystalline phases made by the two copolymers. At low temperatures, the rod-coil diblock copolymers exhibit crystalline and smectic-A phases. The triblock rod-coil copolymers show smectic-C and crystalline phases, in addition to an isotropic phase at high temperatures. The crystalline phase in the triblock is more stable at high T than the diblock. No sharp transition in the orientational order parameter was observed between these two phases. The nematic phase is also suppressed. However, we believe that this phase could show up when the rod-to-coil fraction is increased. This work is in progress. Finally, we should say that our choice of seven DPD particles per rod was because that liquid-crystalline phases of rodlike fluids consisting of less than seven particles was not obtained. However, rod-coil copolymers consisting of six particles per rod and six particles per coil have shown liquid-crystalline ordering of the rods forced by microphase separation.

ACKNOWLEDGMENTS

A. AlSunaidi acknowledges the support from the British Council in Saudi Arabia and King Fahd University of Petroleum and Minerals (KFUPM).

- ¹M. W. Matsen and F. S. Bates, *J. Chem. Phys.* **106**, 2436 (1997).
- ²M. W. Matsen and R. B. Thompson, *J. Chem. Phys.* **111**, 7139 (1999).
- ³S. M. Mai, W. Mingvanish, S. C. Turner, C. Chaibundit, J. Fairclough, F. Heatley, M. Matsen, A. Ryan, and A. Booth, *Macromolecules* **33**, 5124 (2000); C. Chaibundit, W. Mingvanish, S. C. Turner, S. M. Mai, J. Fairclough, A. Ryan, M. Matsen, and A. Booth, *Macromol. Rapid Commun.* **21**, 964 (2000).
- ⁴A. M. Mayes, and M. Olvera de la Cruz, *J. Chem. Phys.* **91**, 7228 (1989); A. M. Mayes, and M. Olvera de la Cruz, *ibid.* **95**, 4670 (1991).
- ⁵B. D. Olsen and R. A. Segalman, *Mater. Sci. Eng. R.* **62**, 37 (2008).
- ⁶J. T. Chen, E. L. Thomas, C. K. Ober, and G.-p. Mao, *Science* **273**, 343 (1996).
- ⁷S. Jenekhe and X. Chen, *Science* **279**, 1903 (1998); S. Jenekhe and X. Chen, *ibid.* **283**, 372 (1999).
- ⁸L. Rubatat, X. Kong, S. A. Jenekhe, J. Ruokolainen, M. Hojiej, and R. Mezzenga, *Macromolecules* **41**, 1846 (2008).
- ⁹M. Lee, B. Cho, H. Kim, J. Yoon, and W. Zin, *J. Am. Chem. Soc.* **120**, 9168 (1998); M. Lee, B. Cho, Y. Jang, and W. Zin, *ibid.* **122**, 7449 (2000).
- ¹⁰M. W. Matsen and C. Barrett, *J. Chem. Phys.* **109**, 4108 (1998).
- ¹¹M. Reenders and G. ten Brinke, *Macromolecules* **35**, 3266 (2002).
- ¹²D. Duchs and D. Sullivan, *J. Phys.: Condens. Matter* **14**, 12189 (2002).
- ¹³R. Hidalgo, D. Sullivan, and J. Chen, *J. Phys.: Condens. Matter* **19**, 376107 (2007).
- ¹⁴J. Chen, C. Zhang, Z. Sun, L. An, and Z. Tong, *J. Chem. Phys.* **127**, 024105 (2007); J. Chen, C. Zhang, Z. Sun, L. An, and Z. Tong, *ibid.* **128**, 074904 (2008).
- ¹⁵J. S. van Duijneveldt, A. Gil-Villegas, G. Jackson, and M. P. Allen, *J. Chem. Phys.* **112**, 9092 (2000).
- ¹⁶H. Fukunaga, J. Takimoto, and M. Doi, *J. Chem. Phys.* **120**, 7792 (2004).
- ¹⁷D. Levesque, M. Mazars, and J. Weis, *J. Chem. Phys.* **103**, 3820 (1995).
- ¹⁸A. Crane, F. Martinez-Veracoechea, F. Escobedo, and E. Muller, *Soft Matter* **4**, 1820 (2008).
- ¹⁹C. McBride and C. Vega, *J. Chem. Phys.* **117**, 10370 (2002).
- ²⁰F. Affouard, F. Kroger, and S. Hess, *Phys. Rev. E* **54**, 5178 (1996).
- ²¹A. Casey and P. Harrowell, *J. Chem. Phys.* **110**, 12183 (1999).
- ²²M. R. Wilson, *J. Chem. Phys.* **107**, 8654 (1997).
- ²³K. Nicklas, P. Bopp, and J. Brickmann, *Chem. Phys.* **101**, 3157 (1994).
- ²⁴L. M. Stimson and M. R. Wilson, *J. Chem. Phys.* **123**, 034908 (2005).
- ²⁵S. Lin, N. Numasawa, T. Nose, and J. Lin, *Macromolecules* **40**, 1684 (2007).
- ²⁶A. AlSunaidi, W. K. den Otter, and J. H. R. Clarke, *Philos. Trans. R. Soc. London, Ser. A* **362**, 1773 (2004).
- ²⁷Y. Levine, A. Gomes, A. Martins, and A. Polimeno, *J. Chem. Phys.* **122**, 144902 (2005).
- ²⁸Z. Hughes, L. Stimson, H. Slim, J. Lintuvuori, J. Illytskyi, and M. R. Wilson, *Comput. Phys. Commun.* **178**, 724 (2008).
- ²⁹W. K. den Otter and J. H. R. Clarke, *Int. J. Mod. Phys. C* **53**, 426 (2001).
- ³⁰R. D. Groot and T. J. Madden, *J. Chem. Phys.* **108**, 8713 (1998).
- ³¹G. Ciccotti, M. Ferrario, and J. P. Ryckaert, *Mol. Phys.* **47**, 1253 (1982).
- ³²M. P. Allen and D. J. Tildesley, *Computer Simulation of Liquids* (Clarendon, Oxford, 1987).
- ³³M. Banaszak and J. H. R. Clarke, *Phys. Rev. E* **60**, 5753 (1999).
- ³⁴M. W. Matsen, *J. Chem. Phys.* **104**, 7758 (1996).
- ³⁵E. de Miguel, E. del Rio, and F. Blas, *J. Chem. Phys.* **121**, 11183 (2004).